ACS OMEGA

http://pubs.acs.org/journal/acsodf

Article

Synthesis, Characterization, Antimicrobial, Density Functional Theory, and Molecular Docking Studies of Novel Mn(II), Fe(III), and Cr(III) Complexes Incorporating 4-(2-Hydroxyphenyl azo)-1-naphthol (Az)

Hany M. Abd El-Lateef,* Mai M. Khalaf, Amer A. Amer, Mahmoud Kandeel, Antar A. Abdelhamid, and Aly Abdou

Cite This: *ACS Omega* 2023, 8, 25877−25891

Read Online

ACCESS | Metrics & More | Article Recommendations | Supporting Information

ABSTRACT: This work synthesized three new $CrAz_2$, $MnAz_2$, and $FeAz_2$ complexes and investigated them using IR, mass, UV spectroscopy, elemental analysis, conductivity and magnetic tests, and thermogravimetric analysis. The azo-ligand, 4-(2-hydroxyphenylAzo)-1-naphthol (Az), couples with metal ions *via* its nitrogen (in −N═N− bonds) and oxygen (in hydroxyl group) atoms, according to the IR spectra of these complexes. Through thermal examination (TG/TGA), the number and location of water in the complexes were also determined. Density functional theory (DFT) theory is applied to ameliorate the structures of the ligand (Az) and metal complexes and analyze the quantum chemical characteristics of these complexes. The antifungal and antibacterial activity of the ligand and its complexes opposed to several hazardous bacteria and fungi was investigated in vitro. Metal complexes were discovered to have a higher inhibitory impact on some organisms than the free ligand. The $MnAz_2$ complex exhibited the best activity among the studied materials, whereas the $CrAz_2$ complex had the lowest. The compounds' binding affinity to the *E. coli* (PDB ID: 1hnj) structure was predicted using molecular docking. Binding energies were calculated by analyzing protein-substrate interactions. These encouraging findings imply that these chemicals may have physiological effects and may be valuable for a variety of medical uses in the future.

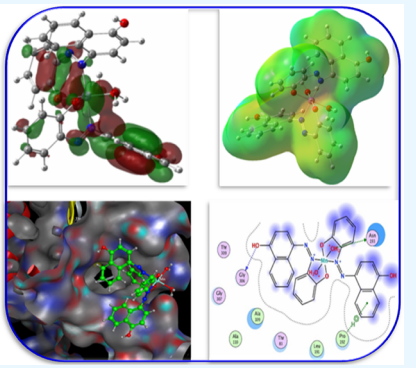

1. INTRODUCTION

Over the course of the past four decades, azo dyes that include heterocyclic rings have made substantial contributions to the field of coordination chemistry.[1] Research in the fields of biology, electrochemistry, and analysis may all make use of these substances in a variety of different ways.[2] Because of their potential cytotoxicity as well as their antibacterial, antifungal, and antioxidant capabilities, they have garnered a lot of studies.[3,4] There has been a significant amount of research done on the production of metal(II) complexes of azo compounds, as well as their biological activity.[5,6] Because their azo group possesses powerful medicinal properties, azo dyes are advantageous chelating agents for a variety of metal ions,[7,8] due to the azo group of these dyes. In addition to this, it has been demonstrated that azo metal complexes can be beneficial as metal anticorrosion agents and as thermally stable optical storage devices,[9,10]

There is an urgent need for new metal-based compounds that can prevent the development of hazardous germs that have become worldwide spread. These microorganisms have the potential to pollute food, water, and soil, as well as cause sickness in humans, animals, and plants.[11,12] In recent years, bioinorganic chemistry, which is the study of coordination chemistry with biological ligands, has experienced tremendous expansion. Bio-metals such as manganese, iron, cobalt, nickel, and copper have been major contributors to this rise. The study of metal-bioligand complexes is essential to gaining an understanding of the processes that occur in living organisms.[13,14] Because coordination chemistry has a history of being successful in the field of pharmacotherapy, academics and researchers have been keenly interested in the topic for a significant amount of time.

Metal ions are selected based on their broad biological history. Previously, complexes of Cr(III), Mn(II), and Fe(III) with azo ligands were reported to show anticancer, antioxidant, and antibacterial activity.[7,15−18] Therefore, we speculate that complexes of Cr(III), Mn(II), and Fe(III) with azo ligands will show more antibacterial and antifungal activity. These findings prompted us to start a project on Cr(III), Mn(II), and Fe(III)-

Received: March 4, 2023
Accepted: July 3, 2023
Published: July 14, 2023

Scheme 1. Preparation of Az Ligands and Its Complexes

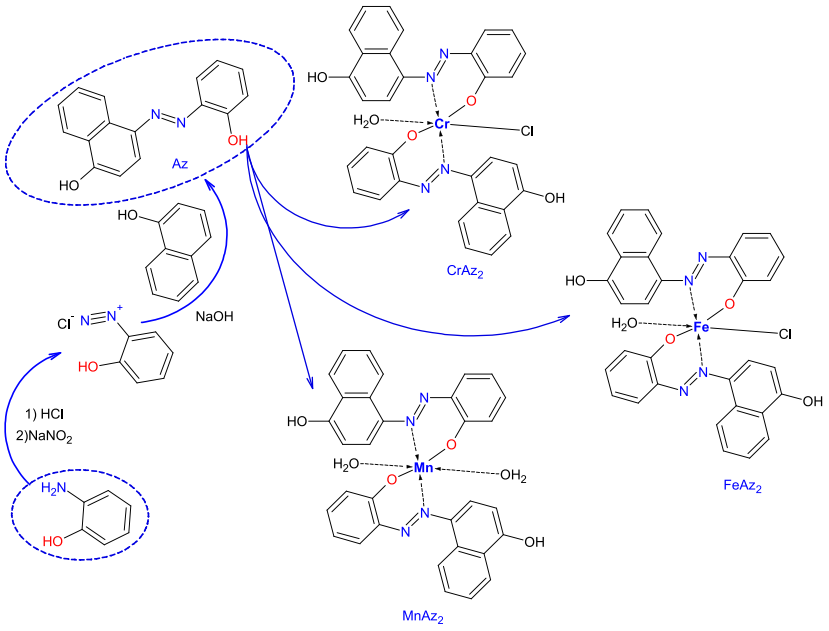

azo-ligand complexes, involving an investigation of their structural characterization, antibacterial, and antifungal properties.

As a result, the purpose of this work is to develop novel coordination compounds based on azo dyes that contain $CrAz_2$, $MnAz_2$, and $FeAz_2$ and then analyze the bioactivity of these compounds in vitro and computationally. In addition, density functional theory (DFT) simulations were utilized so that the three-dimensional (3D) chemical structure of the complexes could be determined. Authors anticipate that the current effort may result in the discovery of a new family of chemicals that due to the ease with which they can be produced and the remarkable efficacy they possess, may represent promising candidates for the treatment of bacterial and fungal diseases.

2. EXPERIMENTAL SECTION

2.1. Synthesis. *2.1.1. Materials and Reagents.* The purity of the chemicals used was suitable for use as analytical reagents (AR). These included 4-(2-hydroxyphenylAzo)-1-naphthol, chromium(III) chloride, manganese(II) chloride, and iron(III) chloride, in addition to organic solvents, such as EtOH and CH_3CN.

2.1.2. Synthesis of the 1-(2-Hydroxyphenylazo)-2-naphthol Azo-Ligand (Az). 1-(2-Hydroxyphenylazo)-2-naphthol as the azo-ligand (Az) was prepared as previously reported[19] with slight modifications.

2.1.2.1. Step I: Preparation of Diazonium Salt of 2-Aminophenolas Azo Molecules. A cooled solution (0 °C) of $NaNO_2$ (0.69 g, 0.01 mol) in 25 mL of water was gradually added to a cooled solution of 1.09 g (0.01 mol) of 2-aminophenol and 36 mL of HCl under stirring in an ice bath for 20 min. The diazonium salt solution was stored in the refrigerator at all times (Scheme 1).

2.1.2.2. Step II: Coupling Procedure. The cooled solution of diazonium salt was gradually added to the cooled solution (0 °C) of 1-naphthol (1.44 g, 0.01 mol) in NaOH (10% w/v) in an ice bath. Then, the azo dye will be precipitated. The final azo product was produced by filtration of the crude precipitate, multiple cold water washes, and recrystallization from the suitable solvent; Scheme 1.

2.1.2.3. 4-(2-Hydroxyphenyl azo)-1-naphthol. Brown−red solid; yield (91%); mp. 190−191 °C; IR (cm^{-1}): 3114−3218 (OH), 3001 (Ar-H); ^{1}H NMR (400 MHz, DMSO-d_6) δ (ppm): 11.25 (s, 1H, OH), 8.56 (s, 1H, OH), 8.26−6.98 (m, 10H, Ar-H); ^{13}C NMR (100 MHz, DMSO-d_6) δ (ppm): 157.99, 154.55, 139.65, 132.84, 128.50, 125.93,123.20, 123.07, 122.43, 120.31, 118.34, 115.53, 109.05; elemental analysis for $C_{16}H_{12}N_2O_2$ (calcd/found); C, 72.72/72.62; H, 4.55/4.41; N, 10.60/10.71.

2.1.3. Preparation of the Metal Complexes. During the process of heating the combination, a solution of the metal salt (2.0 mmol) in water (10 mL) was progressively added to ethanol that already contained the ligand (4.0 mmol). The solution was stirred consistently during the ten-hour process of refluxing in a water bath at 90 °C. The product was recrystallized after it had been filtered, dried, and washed with a water−ethanol mixture with a ratio of 1:2. It was established how much of each product could be obtained as well as the melting and decomposition temperatures; Scheme 1.

2.2. Characterization. The various physicochemical techniques used for the characterization of the free Az ligand and its metal complexes are listed in the Supplementary data file.

2.3. DFT Calculations. To optimize the geometry of the AZ ligand and its complexes, the cc-pVQZ,[20,21] the basis set as a full-electron basis set for all elements composing the investigated compounds in conjunction with the hybrid correlation functional (B3LYP),[22−24] was used in ethanol as the solvent. The solvent (ethanol) effect was solved using the polarizable constant model (IEFPCM).[25,26] The DFT calculations[27] were done using Gaussian 09 W,[28] and the optimized structures, highest occupied molecular orbitals (HOMO)−lowest unoccupied molecular orbitals (LUMO) orbitals, and molecular electrostatic potential (MEP) map were visualized using GaussView 5.[29] Also, natural bond orbital (NBO) analysis of the current compounds was performed

https://doi.org/10.1021/acsomega.3c01413
ACS Omega 2023, 8, 25877−25891

Table 1. Physical Properties, UV−Vis, Conductivity, Magnetic, and FT-IR Results

		Az	$CrAz_2$	$MnAz_2$	$FeAz_2$
physical properties	color	brown−red	white−green	white yellow	dark-violet
	melting point (°C)	190−191	>300	>300	>300
	yield (%)	97	90	87	89
conductivity μ_v, Ω^{-1} cm^2 mol^{-1}	Acetonitrile		11.78	12.04	11.44
	DMF		10.15	9.48	10.07
	assignment		Non-electrolyte		
UV−vis	λ_{max}, nm	380	615	410	505
magnetic	μ_{eff} (B.M)		3.84	1.96	1.84
	assignment		d^3 (t_{2g}^3)	d^5 low spin (t_{2g}^5)	d^5 (t_{2g}^5)
stoichiometry	M:L		1:2	1:2	1:2
IR spectra	υ (−OH)	3318	3478	3488	3460
	υ (−N═N)	1542	1464	1460	1470
	υ (M−O)		551	547	544
	υ (M−N)		485	478	484
EA found (calc.) %	C	72.62 (72.72)	60.47 (60.81)	62.53 (62.24)	60.28 (60.45)
	H	4.41 (4.55)	3.55 (3.83)	4.66 (4.24)	3.66 (3.80)
	N	10.71 (10.60)	8.69 (8.86)	8.87 (9.07)	8.62 (8.81)
	M		8.54 (8.23)	8.72 (8.90)	8.99 (8.78)

using the NBO 3.1 programme[30] as applied in the Gaussian 09 program. To determine quantum chemical parameters such as ionization potential (IP = $-E_{HOMO}$), electronegativity (EN = (I.P. + E.A.)/2), the energy gap ($\Delta E = E_{LUMO} - E_{HOMO}$), chemical potential (CP = −EN), electron affinity (EA = $-E_{LUMO}$), softness ($S = 1/CH$), chemical hardness (CH = (I.P. − E.A.)/2)), and electrophilicity index ($EP = EN^2/2CH$), the LUMO and HOMO energies of the relevant compounds were utilized.[31,32]

2.4. In Vitro Investigation of Bioactivity. The antimicrobials activity of the compounds was examined using the disc diffusion method,[33,34] against a panel of bacteria (*Escherichia coli* (−ve), *Pseudomonas aeruginosa* (−ve), *Bacillus cereus* (+ve), and *Staphylococcus aureus* (+ve)) and fungi. The results showed that the compounds were effective against all of the bacteria and fungi tested (*Trichophyton rubrum*, *Candida albicans*, and *Aspergillus flavus*). The inhibitory zone that surrounded the disc was measured in millimeters and the compounds' activity was compared to that of the standard chloramphenicol antibiotic using the percentage activity index (AI% = IZ of the test compound/IZ of the standard) multiplied by 100.[35,36]

2.5. Molecular Docking. Molecular docking simulations of the specified compounds were performed against the 1HNJ protein to validate the therapeutic efficacy of these compounds. 1HNJ is the structural representation of the FabH-CoA complex in *E. coli*. It is believed that the FabH receptor is targeted with a view to learning about the potential antibacterial properties of chemicals that are present in nature.[37,38] The enzyme FabH plays a role in the synthesis of fatty acids.

The three-dimensional structure of the objective protein receptor was attained by consulting the protein database (http://www.rcsb.org). The chemicals that are researched are utilized as a substrate. The molecular docking investigation is carried out with the use of a molecular overeating environment (MOE).[39]

After creating a new database, optimizing each chemical by reducing the amount of energy required for substrate preparation, and finally storing the results in the MDB format, in order to prepare the receptor, the target receptor underwent processes including the addition of hydrogen atoms, the connection of receptor types, the fixing of potential energy, and, finally, the manufacture of active pockets and dummies.[40,41] Docking patterns and interaction parameters were exported so that interaction features could be analyzed, and inhibitory activity could be ranked according to a scoring function (S, kcal/mol).[42,43]

3. RESULTS AND DISCUSSION

3.1. Structural Configuration of the Azo-Ligand Ligand (Az). The chemical structure of the azo-ligand (Az) was assured by its spectral (IR, ^{1}H NMR, and ^{13}C NMR) and elemental analyses. During the Az analysis, a wide OH absorption band was found between 3114 and 3218 cm^{-1}, and an aromatic C−H band was identified at 3001 cm^{-1}. At 1542 cm^{-1}, the characteristic band that can be produced by the N═N group during stretching vibration absorption was also seen.

Singlet broad signals for the −OH group were seen in the ^{1}H NMR spectra of Az at 11.25 (s, 1H, OH) and 8.56 (s, 1H, OH), as well as aromatic signals at 8.26−6.98 ppm (m, 10H, Ar−H). Signals were seen in the^{13}C NMR spectra at the following frequencies: 157.99, 154.55, 139.65, 132.84, 128.50, 125.93, 123.20, 123.07, 122.43, 120.31, 118.34, 115.53, 109.05 which is characteristic of CH of phenyl and naphthyl moiety, Supporting data; Figure S1. Also, the elemental analysis of the Az ligand referred to good agreement between the found and calculated values for C, H, and N, Table 1, which confirms the proposed structure; Scheme 1.

3.2. Structural Clarification of the Metal Complexes. *3.2.1. Conductivity Measurements and Elemental Analysis.* The metal complexes that are formed are stable even when the temperature is kept at room temperature. Although they are insoluble in water, they are dissolvable in DMF and acetonitrile. The molar conductivity (10^{-3} M in both DMF and acetonitrile solution) as well as the elemental analysis of the generated compounds is displayed in Table 1. The theoretical and experimental elemental analyses of metal complexes are very well in agreement with one another. The proposed formula of the title complexes, from the correlation of the elemental analyses data, are $C_{32}H_{24}ClCrN_4O_5$, $C_{32}H_{26}MnN_4O_6$, and $C_{32}H_{24}ClFeN_4O_5$, for the Cr(III),

https://doi.org/10.1021/acsomega.3c01413
ACS Omega 2023, 8, 25877−25891

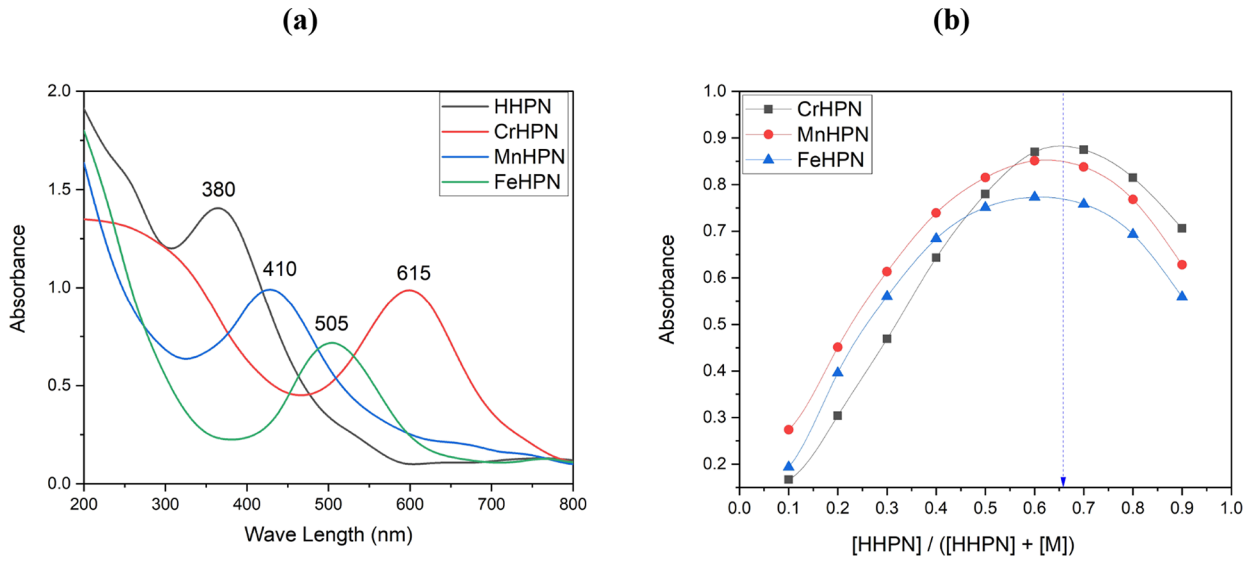

Figure 1. (a) UV−Vis Spectral and (b) stoichiometry of the $CrAz_2$, $MnAz_2$, and $FeAz_2$ complexes.

Mn(II), and Fe(III) complexes, respectively. The metal complexes do not have an electrolytic character, which may be deduced from the low molar conductivity values.

3.2.2. IR Spectra. The purpose of the infrared spectral collection was to achieve a deeper comprehension of the relationship that exists between the Az ligand and the metal ion. The most significant infrared bands that may be used to determine the ligand−metal combination that works best are outlined in Table 1 which can be found here. These bands are almost certainly the result of interactions between the coordinating sites of the ligand and the metal ions in the molecule.

At a frequency of 1542 cm^{-1}, the azo (−N═N−) band was identified. This band showed up in the IR spectra of the Az ligand after coordination with the metal ion, but it did so at a lower wave number, 1460−1470, as shown in Table 1. This indicates that coordination occurred with the azo-nitrogen.

In the infrared spectra of the unbound ligand, the phenolic−OH band could be seen anywhere between 3114 and 3218 cm^{-1} in wavelength. The vibration phenolic−OH was similarly eliminated in the metal complexes, which lends credence to the theory that the phenolic oxygen of the ligand plays a role in the formation of the C−O−M bond during deprotonation;[44,45] Table 1.

The broadband in the complexes was positioned at >3400 cm^{-1}; it was determined that this band was caused by −OH groups on water molecules.[46,47] In addition, the complexes have two additional spectral bands, which may be found at 478−485 and 544−551, respectively, and are referred to as (M−N)[48,49] and (M−O);[50,51] Table 1.

Our research shows that the Azo-ligand, Az, functions as a mononegatively bi-dentate ligand, meaning that it generates complexes by way of both its azo-nitrogen (−N═N−) and phenolic oxygen (−OH) atoms. This is the conclusion that we have drawn from our data.

3.2.3. Magnetic Moment and Electronic Spectra Measurements. The UV−V of the Az ligand and its metal complexes were measured in acetonitrile between 200 and 800 nanometers. Electronic transitions that may be attributed to $n \rightarrow \pi^*$ states were observed to take place in the unbound Az ligand when it was observed at 380 nm. When a metal ion was present, the band shifted to longer wavelengths than it normally would have been. With a view to determining the internal structure of the transition metal complexes, the effective magnetic moment, denoted by the formula $\mu_{eff} = 2.83$ $(((X_g{*}\text{Mwt}) - (\text{dia magnetic correction}{*}T))^{0.5})$, was utilized as another method.

In the case of the $CrAz_2$ complex, the electronic spectrum band at 615 nm was connected to the transition of $^4A_{2g}(F) \rightarrow {}^4T_{2g}(F)$ in the octahedral geometry complex.[52] The 3.84 B.M magnetic moment found for the $CrAz_2$ complex may be described by the occurrence of a d^3 $(t_{2g}{}^3)$ electron configuration in an octahedral geometry around the Cr(III) center. The results from the electronic transitions are supplemented by an effective magnetic moment value (3.84 μ_B), which is within the experimentally acceptable range (3.70−3.90 μ_B) for Cr(III) complexes.[53]

In the case of the $MnAz_2$ complex, the band in its electronic spectra that is located at 24390.24 cm^{-1} may be ascribed to $^6A_{1g}(F) \rightarrow {}^4A_{1g}(G)$ transition, which hints at an octahedral geometry around the Mn(II) center;[54,55] Table 1. The value of 1.96 B.M for the μ_{eff} of the $MnAz_2$ complex is indicative of the occurrence of a d^5 low-spin $(t_{2g}{}^5)$ electron configuration in an octahedral geometry around the center of Mn(II);[56] Table 1.

The electronic spectrum of $FeAz_2$ shows a transition band at 19,801.98 cm^{-1}. This visible band is assigned to the ligand-to-metal charge transfer (LMCT) band characteristic of octahedral iron(III) complexes. In general, high-spin Fe(III) complexes have magnetic moment values of around 5.90 μ_B with no possibility of orbital contribution, while low-spin complexes ($S = 1/2$) have values close to 1.70 μ_B.[57] The μ_{eff} value for $FeAz_2$ is found to be 1.84 μ_B, which is compatible with a return to the d^5 $(t_{2g}{}^5)$ configuration;[58] Table 1. This suggests that the complex has an octahedral geometry with Fe(III) as its core.

3.2.4. Metal Complexes Stoichiometry. The continuous variation method developed by Jobs was applied in the process of determining the chemical formula of metal complexes.[59] The detailed procedures for the Jobs method of continuous variation are listed in the Supporting Information. The absorbance curve that was generated by using this method demonstrated the highest level of absorption at a mole fraction

https://doi.org/10.1021/acsomega.3c01413
ACS Omega 2023, 8, 25877−25891

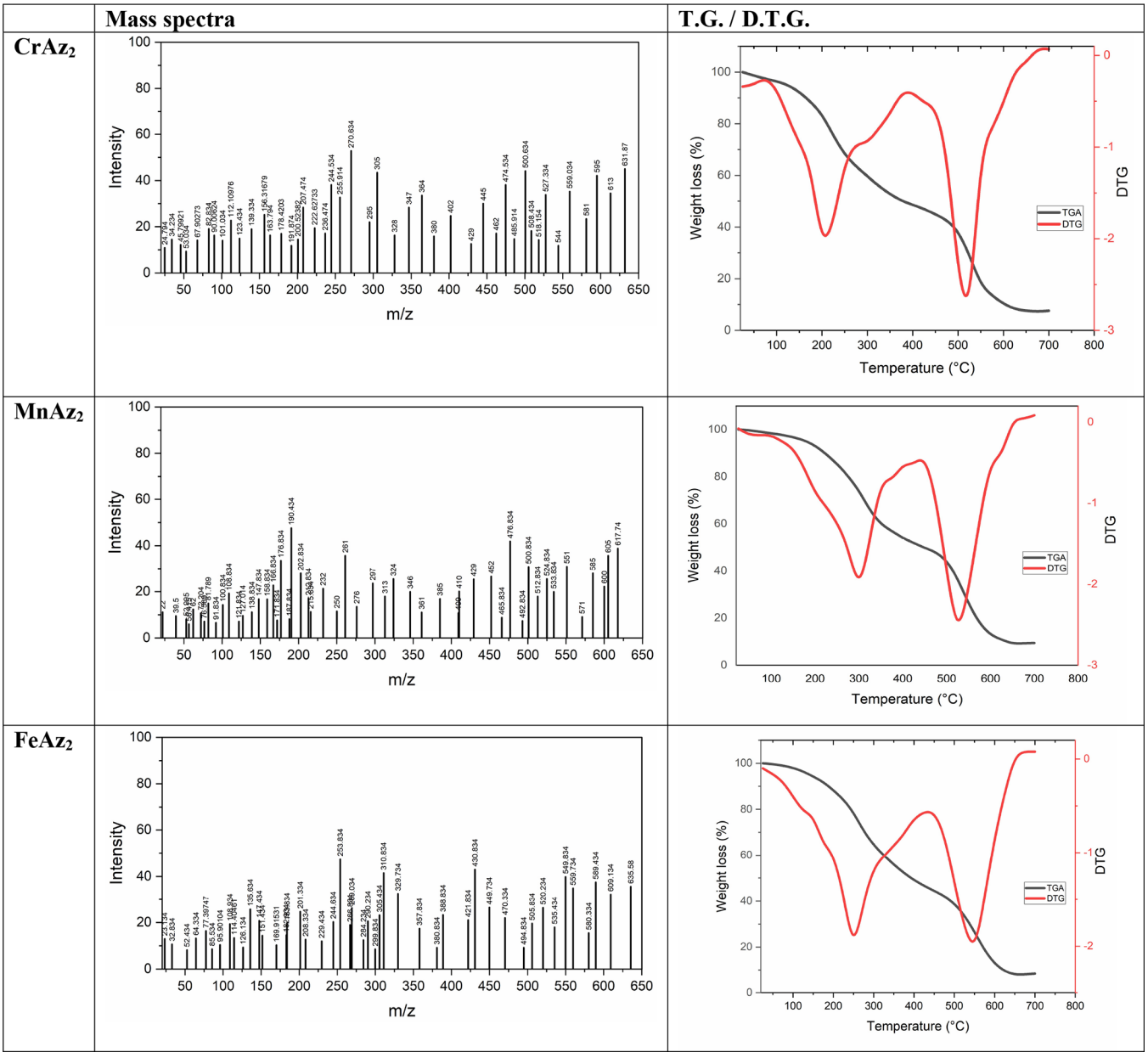

Figure 2. Mass spectra and TG/ DTG curves of the $CrAz_2$, $MnAz_2$, and $FeAz_2$ complexes.

Table 2. Thermal Decomposition of the Prepared Complexes

			mass loss (%)			
	TG (°C)	DTG (°C)	found	calculated	assignment	residue
$CrAz_2$	30–430	215	53.84	53.76	$1H_2O + C_{20}H_{14}O_2Cl$	Cr
	430–650	520	38.22	38.01	$C_{12}H_8O_2N_4$	
$MnAz_2$	30–420	295	52.29	52.19	$2H_2O + C_{20}H_{14}O_2$	Mn
	420–640	530	39.13	38.90	$C_{12}H_8O_2N_4$	
$FeAz_2$	30–440	255	53.24	53.42	$1H_2O + C_{20}H_{14}O_2Cl$	Fe
	440–680	540	37.91	37.77	$C_{12}H_8O_2N_4$	

of the ligand equal to 0.65. This finding hints that the complex was formed with a metal-to-ligand ratio of 1:2 (as seen in Figure 1), as was previously mentioned.

3.2.5. Mass Spectra. The patterns of mass spectra are analyzed to determine the proportional amounts of the constituent parts of a substance. During the course of our investigation, we looked at the mass spectra of several metal complexes, as can be shown in Figure 2. The molecular ion peak, denoted by the symbol M+, can be found in the mass spectra of the $CrAz_2$, $MnAz_2$, and $FeAz_2$ complexes, and its values (631.87, 617.74, and 635.58) are excellent matches for the values that were predicted (631.5, 617, and 635.5). It is possible that the particular characteristics of the metal complexes are responsible for the presence of other peaks in

https://doi.org/10.1021/acsomega.3c01413
ACS Omega 2023, 8, 25877−25891

the mass spectrum. The results of our analysis of the mass spectrum are in line with the previously established values for carbon, hydrogen, and nitrogen, as well as the hypothesized structure.

3.2.6. Thermal Analysis of the Prepared Complexes. It is necessary to ascertain the proportion of coordinated to uncoordinated water molecules in order to get an understanding of the structural transformations that take place in metal complexes as a result of heat treatment (Figure 2 and Table 2).[60,37,61]

The first stage of deterioration was observed at temperatures between 30 and 430 °C, 30 and 420 °C, and 30 and 440 °C, with calculated weight loss percentages of (53.84 (53.76), 52.29 (52.19)), and (37.91 (37.77)) corresponding to the removal of $1H_2O$ + $C_{20}H_{14}O_2Cl$, $2H_2O$ + $C_{20}H_{14}O_2$, and $1H_2O$ + $C_{20}H_{14}O_2Cl$ for $CrAz_2$, $MnAz_2$, and $FeAz_2$ complexes, respectively (Figure 2 and Table 2).

The 2nd degradation step was seen at temperatures ranging from 430 to 650 °C, 420 to 640 °C, and 440 to 680 °C, with calculated weight loss percentages of (38.22 (38.01)), (39.13 (38.90)), and (37.91 (37.77)), which corresponded to the elimination of $C_{12}H_8O_2N_4$ for both $CrAz_2$ and $MnAz_2$ complexes, respectively; Figure 2 and Table 2.

At the conclusion of the thermal degrading process, the metal remained as a metallic residue, as seen in Figure 2 and Table 2. Following analysis of the TG and DTG curves, it was concluded that none of the $CrAz_2$, $MnAz_2$, or $FeAz_2$ complexes contain any water molecules that contribute to their hydration despite the fact that the coordination spheres of the $CrAz_2$, $MnAz_2$, and $FeAz_2$ complexes each contain one, two, and one coordinated water molecules, respectively.

3.3. DFT Calculations. *3.3.1. Geometry Optimization.* The Az free ligand and its metal complexes are shown in Figure 3, each with their optimal structural representations. It was found that all of the $CrAz_2$, $MnAz_2$, and $FeAz_2$ complexes have hexa-coordinate geometry as $[Cr(Az)_2(Cl)(H_2O)]$, $[Mn(Az)_2(H_2O)_2]$, and $[Fe(HPN)_2(Cl)(H_2O)]$. The bond parameters (bond length, bond angles, and dihedral angles) of the free ligand and its metal complexes are found in the supplementary data file (Supporting Information data file).

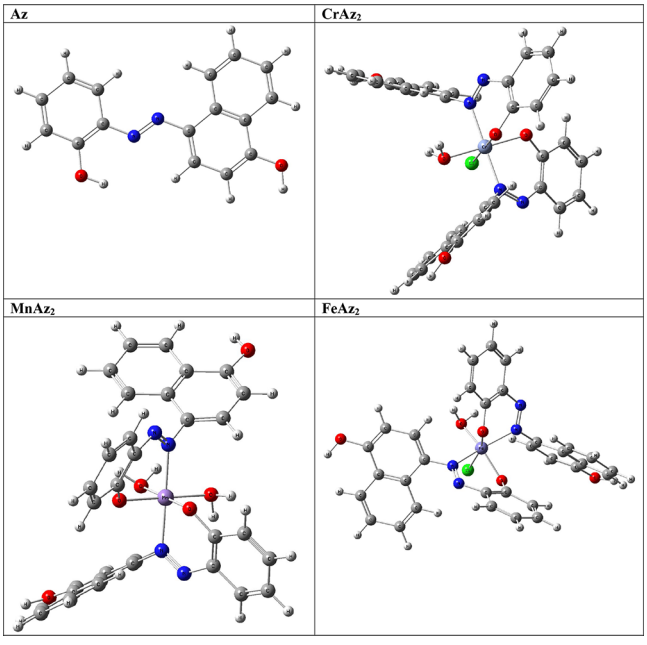

Figure 3. 3D optimized structure of the subject compounds.

The properties in terms of total energy (E_{Total}), energy gap (ΔE), hardness (CH), and softness (S) were calculated for free ligand and compared with that in its metal complexes.

To perform a comparative study of the relative stability of the studied complexes, the binding energy (BE) or the complexation energy of the studied complexes was calculated, Table S1, as follows:[62]

$$E_{binding}\ (\mathrm{Cr(III)\ complex}) = E_{complex} - (E_{Metal\ cation} + 2E_{ligand} + E_{Cl\ anion} + E_{H2O})$$

$$E_{binding}\ (\mathrm{Fe(III)\ complex}) = E_{complex} - (E_{Metal\ cation} + 2E_{ligand} + E_{Cl\ anion} + E_{H2O})$$

$$E_{binding}\ (\mathrm{Mn(II)\ complex}) = E_{complex} - (E_{Metal\ cation} + 2E_{ligand} + 2\,E_{H2O})$$

The more negative BE corresponds to the most stable complex. From the calculated values, Table S1, one can notice that all complexes are more stable than their corresponding ligands, and the order of the complex's stability is $[Fe(HPN)_2(Cl)(H_2O)]$ −692.261 eV) > $[Mn(Az)_2(H_2O)_2]$ (−589.062 eV) > $[Cr(Az)_2(Cl)(H_2O)]$ (−475.781 eV).

3.3.2. Frontier Molecular Orbitals (FMOs) and Reactivity Parameters. The FMOs, especially the HOMOs and the LUMOs, have been widely used to understand the chemical stability, optical, reactivity, and electrical features of various chemical systems.[63,64] The plots of the HOMO and LUMO are provided in Figure 4.

In this particular piece of research, HOMO−LUMO energies were used to calculate a number of different properties, including the energy gap, ionization potential, electronegativity, electron affinity, chemical hardness, chemical potentials, softness, and electrophilicity index. The stability, biological activity, polarizability, reactivity, and hardness−softness of a molecule are all affected by the HOMO and LUMO orbitals.[65,66]

It is also possible to forecast the reactivity of a molecule by making use of the energy gap that exists between these orbitals. As a consequence of this, molecules that have a lower ΔE are more conducive to the docking process ($MnAz_2$ > $FeAz_2$ > $CrAz_2$ > Az).

Hard acids react more frequently with strong bases, whereas soft acids react more frequently with weak bases, according to the hard-soft acid−base rule, which may be used to forecast the chance of one molecule interacting with another. In interactions with biological molecules, soft molecules are preferred over hard molecules, which is to be expected given the prevalence of soft molecules in living things. As a consequence of this, it is possible that soft molecules interact with biological molecules more effectively than hard molecules.[67,68] As a direct consequence of this, the ranking of $MnAz_2$, $FeAz_2$, $CrAz_2$, and Az in Table 3 is as follows: $MnAz_2$ > $FeAz_2$ > $CrAz_2$ > Az.

The chemical potential and electrophilicity index of the compounds in question represent both the substances' inherent stability as well as their predisposition for engaging in the electrophilic activity.[52,69]

https://doi.org/10.1021/acsomega.3c01413
ACS Omega 2023, 8, 25877−25891

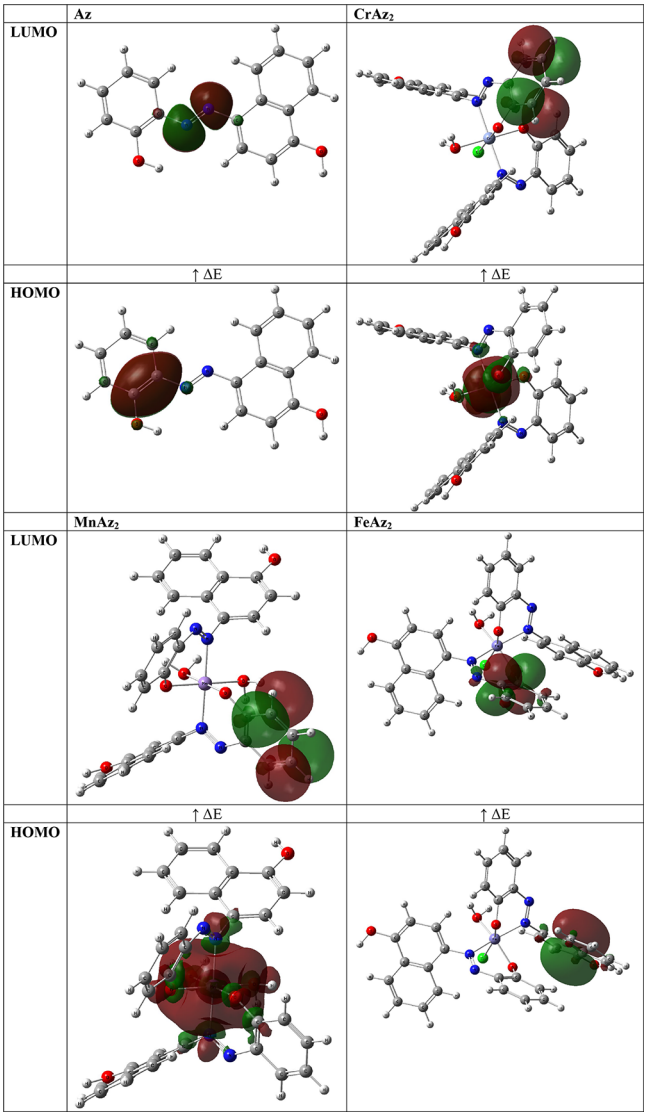

Figure 4. HOMO−LUMO of the optimized structures.

The electrophilicity and nucleophilicity indices are also crucial. The electrophilicity index indicates electron-accepting capacity, whereas the nucleophilicity index demonstrates electron-donating ability.[53,70] As an electrophile, the chemical reactivity ranks in the same direction as a growing electrophilicity index. Thus, in terms of chemical reactivity, $MnAz_2$ is more reactive as an electrophile, followed by $CrAz_2$, than $FeAz_2$ and finally the Az ligand.

3.3.3. Molecular Electrostatic Potential (MEP). Electrostatic potential (MEP) is a measure of the force acting on a positive test charge (a proton) near a molecule due to the electrical charge distribution of the molecule's electrons and nuclei. MEP can be used to visualize the charge distribution of molecules and how they interact with each other. MEP can also be used as a general and versatile indicator for electronic substituent effects in various chemical reactions,[71,72] A color-coded map is used in MEP representations to highlight the various charge values of the electronic potential that was present at the surface of the molecule. These charge values were observed. The region that is lacking electrons is depicted as a positively charged zone in blue, whilst the region that is abundant in electrons is depicted as a negatively charged region in red. The mapping MEP of the compounds under study were explored theoretically and is provided in Figure 5.

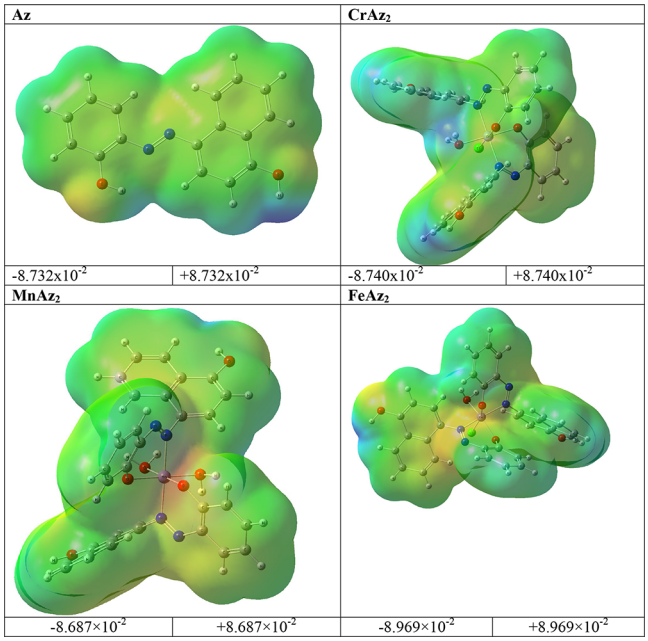

Figure 5. MEP of the title compounds.

In spite of the fact that the majority of the positive sites were found on the hydrogen atoms, while the negative charges were found on hetero oxygen and nitrogen atoms. This indicated that the ligand is an electron donor through the hetero oxygen and nitrogen atoms.

3.3.4. Natural Charge Analysis. Because they represent the physicochemical characteristics of a molecule (the electronic structure, vibrational spectra, dipole moment, polarizability, and other molecular properties), atomic charges play a significant role in molecules,[73,74] The atomic charges of the free ligand and its Cr(III), Mn(II), and Fe(III) complexes in the current investigation were calculated using NBO analysis at the B3LYP/cc-pVQZ level of theory in ethanol as the solvent. The findings are presented in Figure 6 and in the Supporting Information file.

Table 3. Calculated E_{HOMO} (eV), E_{LUMO} (eV), ionization Potential (IP, eV), Electronegativity (EN, eV), the Energy Gap (ΔE, eV), Chemical Potential (CP, eV), electron Affinity (EA, eV), Softness (S, eV), Chemical Hardness (CH, eV), and Electrophilicity Index (EP, eV) of the Subject Compounds

	E_{HOMO} (eV)	E_{LUMO} (eV)	ΔE (eV)	IP (eV)	EA (eV)	EN (eV)	CP (eV)	CH (eV)	S (eV^{-1})	EP (eV)
Az	−10.22	−1.17	9.05	10.22	1.17	5.69	−5.69	4.52	0.11	3.58
$CrAz_2$	−14.10	−8.14	5.96	14.10	8.14	11.12	−11.12	2.98	0.34	20.76
$MnAz_2$	−17.83	−12.35	5.48	17.83	12.35	15.09	−15.09	2.74	0.37	41.58
$FeAz_2$	−10.26	−4.61	5.65	10.26	4.61	7.44	−7.44	2.83	0.35	9.78

https://doi.org/10.1021/acsomega.3c01413
ACS Omega 2023, 8, 25877−25891

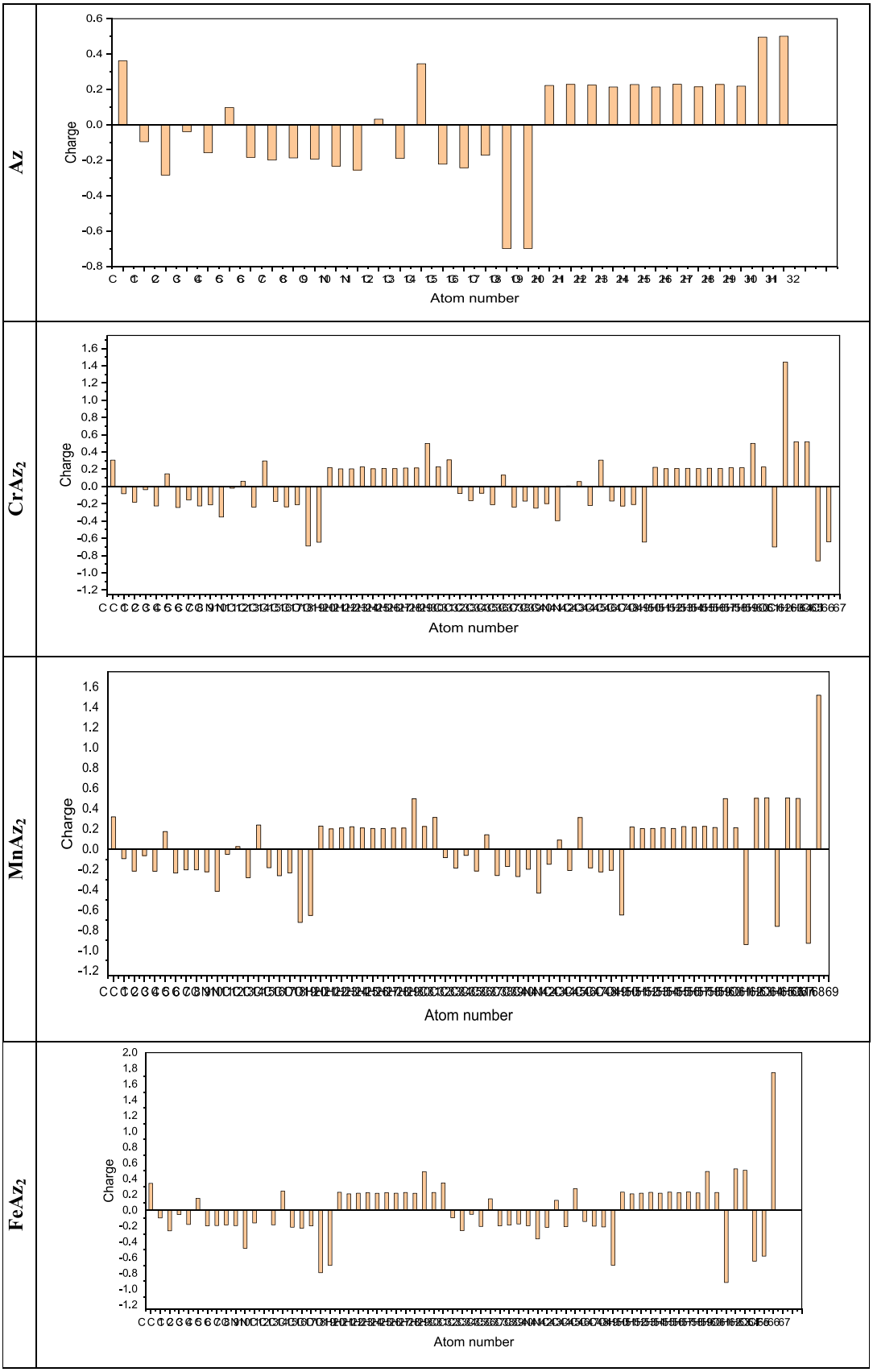

Figure 6. Plot of natural charge distribution of the free ligand and its Cr(III), Mn(II), and Fe(III) complexes computed using the B3LYP/cc-pVQZ level of theory in ethanol as the solvent.

https://doi.org/10.1021/acsomega.3c01413
ACS Omega 2023, 8, 25877−25891

Understanding electronegativity equalization and charge transfer in the chemical reactivity of the title molecules is made easier with the use of NBO analysis. The NBO analysis of the molecules reveals that carbon atoms in the free ligand and its Cr(III), Mn(II), and Fe(III) complexes contain both positive and negative charges. Positive carbons are seen for carbon atoms coupled to the electron-withdrawing oxygen and nitrogen atoms, as illustrated in Figure 6, and the values are tabulated in the Supporting Information file, including (C1, C15, C6, C13), (C32, C46, C1, C15, C6, C37, C13, C44), (C1, C32, C46, C15, C6, C37, C44, C13), and (C32, C1, C46, C15, C6, C37, C44, C13) atoms in the tiled free ligand and its Cr(III), Mn(II), and Fe(III) complexes, respectively. On the other hand, the other carbon atoms including carbon atoms (C3, C17, C16, C8, C10, C14, C9, C7, C18, C5, C2, C4), (C40, C7, C38, C14, C17, C48, C5, C9, C45, C10, C18, C36, C49, C41, C3, C16, C39), (C14, C40, C17, C38, C7, C18, C48, C10, C5, C3, C36, C45, C49, C8, C9, C41, C34), and (C3, C34, C17, C16, C49, C45, C36, C48, C38, C7, C18, C41, C10, C8, C39) have a negative charge in the tiled free ligand and its Cr(III), Mn(II), and Fe(III) complexes, respectively. More specifically, the C1 (0.36179 e), C32 (0.30866 e), C1 (0.31891 e), and C32 (0.34781 e) atoms are the largest positive carbons, while the carbon atoms C3 (−0.28405 e), C40 (−0.25088 e), C14 (−0.28139 e), C3 (−0.25998 e) atoms are the largest negative carbons, for the free ligand and its Cr(III), Mn(II), and Fe(III) complexes, respectively. All the hydrogen atoms in the free ligand and its Cr(III), Mn(II), and Fe(III) complexes have positive charges. Specifically, the H32 (0.50109 e), H65 (0.51891 e), H64 (0.50612 e), H63 (0.52542 e) atoms are the positive hydrogen atoms in the free ligand and its Cr(III), Mn(II), and Fe(III) complexes, respectively.

The net charges of the Cr(III), Mn(II), and Fe(III) ions in the Cr(III), Mn(II), and Fe(III) complexes are (1.4412 e), (1.51852 e), and (1.74594 e), respectively, whereas the valence of the free Cr(III), Mn(II), and Fe(III) ions is +3, +2, and +3, respectively. The decrease in the positive charge of the Cr(III), Mn(II), and Fe(III) ions in the Cr(III), Mn(II), and Fe(III) complexes was due to accumulation of the electronic charges from the associated coordinated ions.

3.3.5. NBO Analysis. The NBO study gives evidence for interactions between donors and acceptors and predicts the energy required for their stabilization with second-order perturbations.[75] In order to demonstrate the donor−acceptor interactions that take place between the HOMO and LUMO levels of the molecule, the NBO analysis was carried out using the B3LYP/cc-pVQZ method. Supporting Information data provide a summary of the natural population analysis that was calculated as well as the natural electronic configuration of the investigated compounds.

The NBO method is well recognized as a fast approach to learning about the features of the electronic structure. Donor−acceptor analysis is facilitated by this method, as is analysis of charge transfer, delocalization, and conjugative interactions in molecules.[76]

The NBO analysis tool is a helpful method for investigating charge transfer or hyper-conjugative interactions, as well as for analyzing intra- and intermolecular bonding. The NBO quantitatively examines bonding and anti-bonding interactions caused by second-order disturbance by expressing the energy of these interactions as $E^{(2)}$.[77−79] To calculate the off-diagonal NBO matrix element $E^{(2)} = \Delta E_{ij} = qi(F(i,j)2/E_j - E_i)$, where E_i and E_j are the diagonal elements, qi is donor orbital occupancy and $F_{i,j}$ is the NBO off-diagonal matrix element.

According to observations of perturbation energy $E^{(2)}$ for various transitions between these donors and acceptors, the Supporting Information file, the following transitions for free ligands are extremely likely to occur; for free ligands; C1−C3 → C2−C4 (132.62 kJ/mol, $\pi \rightarrow \pi^*$), C13−C15 → C17−C18 (116.7 kJ/mol, $\pi \rightarrow \pi^*$), C13−C15 → C14−C16 (76.25 kJ/mol, $\pi \rightarrow \pi^*$), O19 → C13−C15 (27.81 kJ/mol, LP → π^*), for Cr(II) complex; C7−C8 → C9−C10 (88.93 kJ/mol, $\pi \rightarrow \pi^*$), C35−C37 → C40−C41 (53.76 kJ/mol, $\pi \rightarrow \pi^*$), C1−C2 → C7−C8 (41.96 kJ/mol, $\pi \rightarrow \pi^*$), C4−C6 → C9−C10 (38.89 kJ/mol, $\pi \rightarrow \pi^*$), for Mn(II) complex; C1−C2 → C4−C6 (720.14 kJ/mol, $\pi \rightarrow \pi^*$), C32−C33 → C35−C37 (400.09 kJ/mol, $\pi \rightarrow \pi^*$), C34−C36 → C35−C37 (338.46 kJ/mol, $\pi \rightarrow \pi^*$), C44−C46 → C45−C47 (62.76 kJ/mol, $\pi \rightarrow \pi^*$), for Fe(III) complex; C13−C15 → C17−C18 (82.91 kJ/mol, $\pi \rightarrow \pi^*$), C13−C15 → C14−C16 (62.76 kJ/mol, $\pi \rightarrow \pi^*$), C44−C46 → C45−C47 (44.13 kJ/mol, $\pi \rightarrow \pi^*$), C44−C46 → C48−C49 (38.44 kJ/mol, $\pi \rightarrow \pi^*$), are the most probable transitions.

Using NBO calculations, significant knowledge on the structures and characteristics of the Cr(III), Mn(II), and Fe(III) complexes was collected. The NBO analysis of the compounds indicated substantial inter- and intramolecular interactions between the acceptor NBOs and the donor NBOs. These interactions were between the donor NBOs and the acceptor NBOs.

3.4. In Vitro Antimicrobial Activity. The newly synthesized compounds' antibacterial and antifungal activity was tested against a diversity of types of bacteria and fungi strains, such as *Pseudomonas aeruginosa*, *Staphylococcus aureus*, *Escherichia coli*, *Aspergillus flavus*, *Bacillus cereus*, *Trichophyton rubrum*, and *Candida albicans*. The purpose of these tests was to gain a better understanding of the newly synthesized compounds. The biological activity of each compound was evaluated by determining how much of an impact it had on the size of the inhibition zone (IZ). This zone serves as a measurement of how effective the chemical is in inhibiting the development of microorganisms. Table 4 demonstrates that the metal complexes had an inferior minimum inhibitory concentration (MIC) and a broader inhibition zone compared to the pristine ligand.

The chelation hypothesis[80−82] proposes that metal ions have a positive charge that can be neutralized through the process of chelation or the creation of a complex with a ligand. This theory is one of several that have been proposed as potential explanations for this phenomenon. This electron delocalization across the ring might make the molecule more lipophilic, which would make it easier for it to enter the lipid bilayer that makes up the cell membrane. Once inside, the complex may cause the binding sites to become unstable and may change the metabolic pathways, which may ultimately result in the bacterium's death.

The inhibition zone values of the newly found compounds are compared in Table 4 with those of the chloramphenicol antibiotic, which has a high activity index and is therefore expected to have a high inhibition zone value. Strong antibacterial activity was shown by the $MnAz_2$ complex against *Escherichia coli* (−ve), *Pseudomonas aeruginosa* (−ve), *Bacillus cereus* (+ve), and *Staphylococcus aureus* (+ve), respectively, with the activity index (%) of 88.89, 83.33, and 90.00, respectively. Additionally, it demonstrated significant antifungal effective-

https://doi.org/10.1021/acsomega.3c01413
ACS Omega 2023, 8, 25877−25891

Table 4. Anti-Bacterial and Anti-Fungal Activity of the Titled Compounds in Terms of Inhibition Zone (IZ, mm) and Activity Index (%)

anti-bacterial activity					
bacterial strains		Az	$CrAz_2$	$MnAz_2$	$FeAz_2$
Pseudomonas aeruginosa	IZ	9	15	16	16
	%	50.00	83.33	88.89	88.89
	MIC	50	12.5	6.25	6.25
Escherichia coli (−ve)	IZ	9	17	18	17
	%	45.00	85.00	90.00	85.00
	MIC	25	6.25	6.25	6.25
Staphylococcus aureus (+ve)	IZ	8	15	15	15
	%	44.44	83.33	83.33	83.33
	MIC	25	12.5	6.25	6.25
Bacillus cereus (+ve)	IZ	9	14	15	14
	%	50.00	77.78	83.33	77.78
	MIC	50	6.25	6.25	6.25
anti-fungal activity					
fungal strains		Az	$CrAz_2$	$MnAz_2$	$FeAz_2$
Aspergillus flavus	IZ	9	16	16	16
	%	47.37	84.21	84.21	84.21
	MIC	25	12.5	6.25	6.25
Trichophyton rubrum	IZ	9	17	18	17
	%	40.91	77.27	81.82	77.27
	MIC	50	12.5	6.25	12.5
Candida albicans	IZ	9	17	17	17
	%	42.86	80.95	80.95	80.95
	MIC	50	12.5	6.25	6.25

ness against *Trichophyton rubrum*, *Aspergillus flavus*, and *Candida albicans*, with activity indexes (%) of 81.82, 84.21, and 80.95, respectively.

The MIC also known as the lowermost dose of a drug that may prevent the growth of bacteria or fungus is frequently used as a starting point in larger preclinical trials of potential antibacterial drugs. These trials are often conducted in preparation for clinical testing. The MIC value was found by repeatedly diluting a sample until the desired concentration was reached. The MIC values that were calculated for the drugs being studied are presented in Table 4. This table demonstrates that the metal complexes had a lower MIC (about 6.25 ppm) than the free ligand did (approximately 50 ppm).

To make a comparison between the biological activity of the compounds that are the subject of this research and that of the metal complexes that have been described in the previous scientific literature,[83−89] Supporting Information; Table S2. The findings indicated that the current compounds had significant values of biological activity which suggests that they could be effective antimicrobials.

3.5. Molecular Docking. To provide a deep understanding of the interactions between the synthesized complexes and target protein *E. coli* (PDB ID: 1hnj), we performed the molecular docking study by using the MOE program. The docking score (*S*) and hydrogen bonding (H) interactions were visualized, and interaction energies were calculated for the title complexes. The obtained energy results are presented in Table 5. Figure 7 demonstrates the structures of synthesized complexes interacting with amino-acid residues through some hydrogen bonding interactions. The significance of the metal ion and ligand is figured out by the energy values of hydrogen bonding interactions forming between the same amino-acid residues and noncoordinated parts of ligands around metal ions.[90,49]

The docking data showed that the active site of the protein had strong interactions with the substrates, including hydrophobic and hydrogen bonding interactions.[91] After all the compounds were investigated, it was found that $MnAz_2$ had the greatest capacity to inhibit, followed by $FeAz_2$, $CrAz_2$, and Az. As can be seen in Table 5 and Figure 7, the most efficient molecule, MnAz2, interacted with the protein through the formation of hydrogen bonds as well as hydrophobic interactions.

The inhibition constant, often known as the *Ki* value, of a molecule, can be utilized to evaluate the drug's potential as a hit, lead, or therapeutic candidate.[92,93] A higher *Ki* rating denotes a more powerful action, which is advantageous because of its increased potency. Throughout the course of this study, the *Ki* values for the compounds ranged anywhere from 1.43 for $MnAz_2$ to 4.85 for $CrAz_2$. According to these data, $MnAz_2$ appears to be a potential therapy method due to the fact that it has a low *Ki* value.

The findings indicate that molecular docking may be used to predict chemical binding affinity to an antimicrobial target protein and provide potential treatment choices. In general, these findings illustrate that molecular docking can be used. These findings will need to be validated via more research and the efficacy of these chemicals as potential medicines will also need to be evaluated.

4. CONCLUSIONS

In this work, we synthesized $CrAz_2$, $MnAz_2$, and $FeAz_2$ complexes and thoroughly analyzed them using a variety of spectroscopic and physicochemical methods. The Az ligand acted as a monobasic bi-dentate NO ligand with 1:2 molar ratios when attached to Cr(III), Mn(II), and Fe(III). Several analytical and spectroscopic techniques were employed to ascertain the geometric structures of the $CrAz_2$, $MnAz_2$, and

Table 5. Molecular Docking Data

	ligand	receptor	interaction	distance	*E* (kcal/mol)	*S* (kcal/mol)	*Ki* (μM)
Az	O 19	THR 81	H-donor	2.85	−1.40	−6.55	16.17
$CrAz_2$	C 5	LEU 191	H-donor	3.21	−0.80	−7.26	4.85
	O 65	LEU 191	H-donor	2.65	−5.10		
$MnAz_2$	O 20	GLY 06	H-donor	2.90	−0.90	−7.98	1.43
	O 65	ASN 193	H-donor	2.66	−12.60		
	6-ring	PRO 192	pi−H	3.62	−0.70		
$FeAz_2$	O 52	THR 81	H-donor	2.90	−2.50	−7.88	1.69
	6-ring	ALA 09	pi-H	3.81	−0.60		

https://doi.org/10.1021/acsomega.3c01413
ACS Omega 2023, 8, 25877−25891

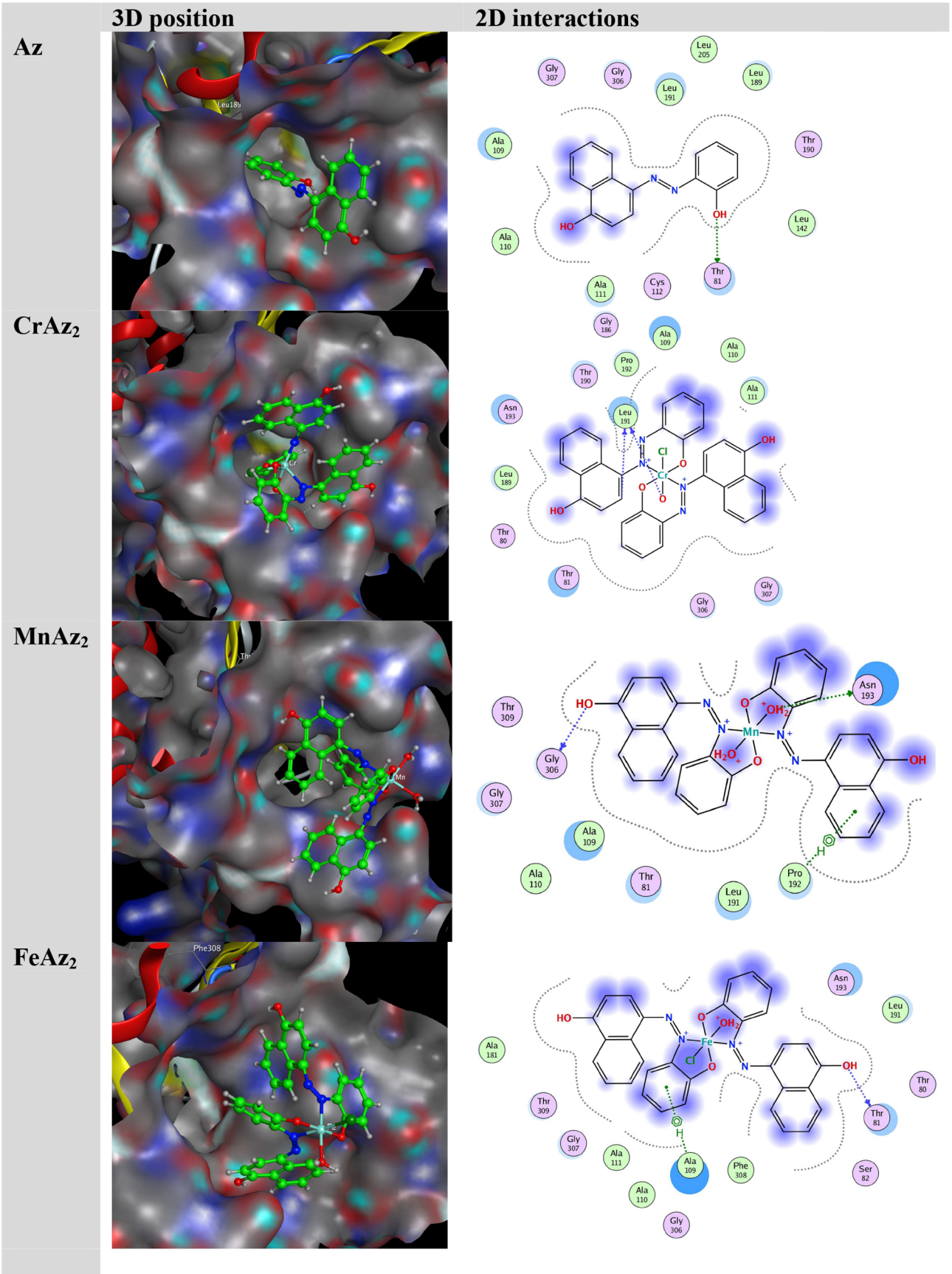

Figure 7. 3D orientation of the substrate−protein complex.

https://doi.org/10.1021/acsomega.3c01413
ACS Omega 2023, 8, 25877−25891

$FeAz_2$ complexes. Our results showed that the $CrAz_2$, MnAz2, and $FeAz_2$ complexes all have octahedral geometries. To further our understanding of the properties of the $CrAz_2$, $MnAz_2$, and $FeAz_2$ complexes, we also used quantum chemistry methods to estimate their theoretically perfect molecular structures. As a result, we were able to foresee and verify the electronic structures of these complexes, which shed light on their prospective medicinal chemistry uses. In addition to analyzing the properties of the free ligand and its metal complexes, we looked into their potential antibacterial and antifungal effects. To test the effects of the free ligand and its metal complexes, we used pathogenic bacterial and fungal strains that are frequently found in Egypt's polluted environments. Based on the results, metal complexes have the potential to be used as efficient antimicrobial agents as they are more active against bacteria than the free ligand. At last, we used molecular docking to examine whether or not the free ligand and its metal complexes were effective in restraining *E. coli* growth (PDB ID: 1hnj). By testing several compounds, we were able to see if any of them were able to bind to the receptor of interest and perhaps alter its function. One of the most promising strategies for inhibiting *E. coli* growth is the $MnAz_2$ complex, which has the highest affinity to the receptor. Our study has elucidated the structure and antimicrobial activity of $CrAz_2$, $MnAz_2$, and $FeAz_2$ complexes in great detail. Having this information can help researchers create and perfect these complexes for use in medicinal chemistry.

■ ASSOCIATED CONTENT

Data Availability Statement

The datasets supporting this article have been uploaded as part of the electronic Supplementary Material.

Supporting Information

The Supporting Information is available free of charge at https://pubs.acs.org/doi/10.1021/acsomega.3c01413.

^{1}H NMR of the AZ free ligand; ^{13}C NMR of the AZ free ligand; binding energy of the studied complexes based on DFT/B3LYP with the cc-PVQZ basis set in ethanol as the solvent; comparison between the minimum inhibition concentrations (MIC) of the current compounds with previously reported compounds in the literature survey against *E. coli*; bond parameters (bond length, bond angles, and dihedral angles) of the free ligand and its metal complexes; summary of natural population analysis; NBO data of the ligand; summary of natural population analysis of the Cr(III) complex; NBO data of the Cr(III) complex; summary of Natural Population Analysis of the Mn(II) complex; NBO data of the Mn(II) complex; summary of natural population analysis of the Fe(III) complex; and NBO data of the Fe(III) complex (PDF)

■ AUTHOR INFORMATION

Corresponding Author

Hany M. Abd El-Lateef − *Department of Chemistry, College of Science, King Faisal University, Al-Ahsa 31982, Saudi Arabia; Chemistry Department, Faculty of Science, Sohag University, Sohag 82524, Egypt;* orcid.org/0000-0002-6610-393X; Email: hmahmed@kfu.edu.sa, Hany_shubra@science.sohag.edu.eg

Authors

Mai M. Khalaf − *Department of Chemistry, College of Science, King Faisal University, Al-Ahsa 31982, Saudi Arabia; Chemistry Department, Faculty of Science, Sohag University, Sohag 82524, Egypt*

Amer A. Amer − *Chemistry Department, Faculty of Science, Sohag University, Sohag 82524, Egypt;* orcid.org/0000-0001-7112-9918

Mahmoud Kandeel − *Department of Biomedical Sciences, College of Veterinary Medicine, King Faisal University, 31982 Al-Ahsa, Saudi Arabia; Department of Pharmacology, Faculty of Veterinary Medicine, Kafrelsheikh University, 33516 Kafrelsheikh, Egypt*

Antar A. Abdelhamid − *Chemistry Department, Faculty of Science, Sohag University, Sohag 82524, Egypt; Chemistry Department, Faculty of Science, Albaha University, Albaha 1988, Saudi Arabia*

Aly Abdou − *Chemistry Department, Faculty of Science, Sohag University, Sohag 82524, Egypt;* orcid.org/0000-0002-5979-2650

Complete contact information is available at: https://pubs.acs.org/10.1021/acsomega.3c01413

Author Contributions

H.M.A.E.-L.: Investigation, Funding acquisition, Writing-original draft, Writing-review and editing. M.M.K.: Investigation, Methodology, Resources, Formal analysis, Data curation, Funding acquisition, Writing-original draft, Writing-review and editing. M.K.: Writing-original draft, Writing-review and editing. A.A.: Investigation, Supervision, Methodology, Resources, Formal analysis, Data curation, Funding acquisition, Writing-original draft, Writing-review and editing. A.A.A.: Investigation, Supervision, Methodology, Resources, Formal analysis, Data curation, Funding acquisition, Writing-original draft, Writing-review and editing. A.A.A.: Investigation, Supervision, Methodology, Resources, Formal analysis, Data curation, Funding acquisition, Writing-original draft, Writing-review and editing. All authors have read and agreed to the published version of the manuscript.

Funding

This work was funded by the Deanship of Scientific Research, at King Faisal University, Saudi Arabia (GRANT 3191).

Notes

The authors declare no competing financial interest.

■ ACKNOWLEDGMENTS

The authors acknowledge the Deanship of Scientific Research, Vice Presidency for Graduate Studies and Scientific Research at King Faisal University, Saudi Arabia, for financial support under the annual funding track (GRANT 3191).

■ REFERENCES

(1) Abouzayed, F. I.; Abouel-Enein, S. A.; Hammad, A. M. Synthesis of Some Novel Nanosized Chelates of Anchoring Bisazo Dye 5-[5-(4, 6-Dioxo-2-thioxo-hexahydro-pyrimidin-5-ylazo)-naphthalen-1-ylazo]-2-mercapto-1 H-pyrimidine-4, 6-dione and Their Applications as Antioxidant and Antitumor Agents. *ACS Omega* **2021**, *6*, 27737−27754.

(2) Nguyen, T. L.; Gigant, N.; Joseph, D. Advances in direct metal-catalyzed functionalization of azobenzenes. *ACS Catal.* **2018**, *8*, 1546−1579.

(3) Eltaboni, F.; Bader, N.; El-Kailany, R.; Elsharif, N.; Ahmida, A. Chemistry and Applications of Azo Dyes: A Comprehensive Review. *J. Chem. Rev.* **2022**, *4*, 313−330.
(4) Bakr, E. A.; Atteya, E. H.; Al-Hefnawy, G. B.; El-Attar, H. G.; El-Gamil, M. M. A novel azo-azomethine benzoxazole-based ligand and its transition metal (II),(III),(IV) complexes: Synthesis, characterization, theoretical studies, biological evaluation, and catalytic application. *Appl. Organomet. Chem.* **2023**, *37*, No. e7042.
(5) Kumar, S. S.; Sadasivan, V.; Meena, S. S.; Sreepriya, R.; Biju, S. Synthesis, structural characterization and biological studies of Ni (II), Cu (II) and Fe (III) complexes of hydrazone derived from 2-(2-(2, 2-dimethyl-4, 6-dioxo-1, 3-dioxan-5-ylidene) hydrazinyl) benzoic acid. *Inorg. Chim. Acta.* **2022**, *536*, No. 120919.
(6) Mehrparvar, S.; Scheller, Z. N.; Wölper, C.; Haberhauer, G. Design of azobenzene beyond simple on−off behavior. *J. Am. Chem. Soc.* **2021**, *143*, 19856−19864.
(7) Deghadi, R. G.; Mahmoud, W. H.; Mohamed, G. G. Metal complexes of tetradentate azo-dye ligand derived from 4, 4′-oxydianiline: Preparation, structural investigation, biological evaluation and MOE studies. *Appl. Organomet. Chem.* **2020**, *34*, No. e5883.
(8) Kongot, M.; Reddy, D. S.; Singh, V.; Patel, R.; Singhal, N. K.; Kumar, A. A manganese (II) complex tethered with S-benzyldithiocarbazate Schiff base: Synthesis, characterization, in-vitro therapeutic activity and protein interaction studies. *Spectrochim. Acta, Part A* **2020**, *231*, No. 118123.
(9) Yousef, T.; Khairy, M. Synthesis, Characterization, Optical, DFT, TD DFT Studies and In silico ADME Predictions of Thiosemicarbazone ligand and its Au (III) Complex. *Orient. J. Chem.* **2022**, *38*, No. 380303.
(10) Wang, M.; Zhao, Y.; Chang, M.; Ding, B.; Deng, X.; Cui, S.; Hou, Z.; Lin, J. Azo initiator loaded black mesoporous titania with multiple optical energy conversion for synergetic photo-thermal-dynamic therapy. *Appl. Mater. Interfaces* **2019**, *11*, 47730−47738.
(11) Elkanzi, N. A.; Hrichi, H.; Salah, H.; Albqmi, M.; Ali, A. M.; Abdou, A. Synthesis, physicochemical properties, biological, molecular docking and DFT investigation of Fe (III), Co (II), Ni (II), Cu (II) and Zn (II) complexes of the 4-[(5-oxo-4, 5-dihydro-1, 3-thiazol-2-yl) hydrazono] methyl} phenyl 4-methylbenzenesulfonate Schiff-base ligand. *Polyhedron* **2023**, *230*, No. 116219.
(12) Alghuwainem, Y. A.; Abd El-Lateef, H. M.; Khalaf, M. M.; Abdelhamid, A. A.; Alfarsi, A.; Gouda, M.; Abdelbaset, M.; Abdou, A. Synthesis, structural, DFT, antibacterial, antifungal, anti-inflammatory, and molecular docking analysis of new VO (II), Fe (III), Mn (II), Zn (II), and Ag (I) complexes based on 4-((2-hydroxy-1-naphthyl) azo) benzenesulfonamide. *J. Mol. Liq.* **2023**, *369*, No. 120936.
(13) Rana, M.; Cho, H.-J.; Roy, T. K.; Mirica, L. M.; Sharma, A. K. Azo-dyes based small bifunctional molecules for metal chelation and controlling amyloid formation. *Inorg. Chim. Acta* **2018**, *471*, 419−429.
(14) Badea, M.; Emandi, A.; Marinescu, D.; Cristurean, E.; Olar, R.; Braileanu, A.; Budrugeac, P.; Segal, E. Thermal stability of some azo-derivatives and their complexes. *J. Therm. Anal. Calorim.* **2003**, *72*, 525−531.
(15) Khedr, A. M.; El-Ghamry, H. A.; El-Sayed, Y. S. Nano-synthesis, solid-state structural characterization, and antimicrobial and anticancer assessment of new sulfafurazole azo dye-based metal complexes for further pharmacological applications. *Appl. Organomet. Chem.* **2022**, *36*, No. e6548.
(16) Mahmoud, W. H.; Sayed, F. N.; Mohamed, G. G. Azo dye with nitrogen donor sets of atoms and its metal complexes: synthesis, characterization, DFT, biological, anticancer and Molecular docking studies. *Appl. Organomet. Chem.* **2018**, *32*, No. e4347.
(17) Mahmoud, W. H.; Sayed, F. N.; Mohamed, G. G. Synthesis, characterization and in vitro antimicrobial and anti-breast cancer activity studies of metal complexes of novel pentadentate azo dye ligand. *Appl. Organomet. Chem.* **2016**, *30*, 959−973.
(18) Saad, F. A.; Elghalban, M. G.; El-Metwaly, N. M.; El-Ghamry, H.; Khedr, A. M. Density functional theory/B3LYP study of nanometric 4-(2, 4-dihydroxy-5-formylphen-1-ylazo)-N-(4-methyl-pyrimidin-2-yl) benzenesulfonamide complexes: Quantitative structure−activity relationship, docking, spectral and biological investigations. *Appl. Organomet. Chem.* **2017**, *31*, No. e3721.
(19) Mohammed, H. Synthesis, identification, and biological study for some complexes of azo dye having theophylline. *Sci. World J.* **2021**, *2021*, No. 9943763.
(20) Wiberg, K. B. Basis set effects on calculated geometries: 6-311++ G** vs. aug-cc-pVDZ. *J. Comput. Chem.* **2004**, *25*, 1342−1346.
(21) Martin, J. M.; Taylor, P. R. Basis set convergence for geometry and harmonic frequencies. Are h functions enough? *Chem. Phys. Lett.* **1994**, *225*, 473−479.
(22) Becke, A. D. Density-functional exchange-energy approximation with correct asymptotic behavior. *Phys. Rev. A* **1988**, *38*, 3098.
(23) Lee, C.; Yang, W.; Parr, R. G. Development of the Colle-Salvetti correlation-energy formula into a functional of the electron density. *Phys. Rev. B* **1988**, *37*, 785.
(24) Raghavachari, K. Perspective on "Density functional thermochemistry. III. The role of exact exchange" Becke AD (1993) J Chem Phys 98: 5648−52. *Theor. Chem. Acc.* **2000**, *103*, 361−363.
(25) Khodiev, M.; Holikulov, U.; Jumabaev, A.; Issaoui, N.; Lvovich, L. N.; Al-Dossary, O. M.; Bousiakoug, L. G. Solvent effect on the self-association of the 1, 2, 4-triazole: A DFT study. *J. Mol. Liq.* **2023**, *382*, No. 121960.
(26) Pecul, M.; Lamparska, E.; Cappelli, C.; Frediani, L.; Ruud, K. Solvent effects on Raman optical activity spectra calculated using the polarizable continuum model. *J. Phys. Chem. A.* **2006**, *110*, 2807−2815.
(27) Kohn, W.; Sham, L. J. Self-consistent equations including exchange and correlation effects. *Phys. Rev.* **1965**, *140*, A1133.
(28) Tomberg, A. Gaussian 09w tutorial. In *An introduction to computational chemistry using G09W and Avogadro software*, 2013; pp 1−36.
(29) Nielsen, A.; Holder, A. *Gauss view 5.0, user's reference*; GAUSSIAN Inc.: Pittsburgh, 2009.
(30) Tian, L.; Feiwu, C. Multiwfn: A Multifunctional Wavefunction Analyzer. *J. Comput. Chem.* **2012**, *33*, 580.
(31) Seleem, H.; El-Shetary, B.; Shebl, M. Synthesis and characterization of a novel series of metallothiocarbohydrazone polymers and their adducts. *Heteroat. Chem.* **2007**, *18*, 100−107.
(32) Shokr, E. K.; Kamel, M. S.; Abdel-Ghany, H.; Ali El-Remaily, M. A. E. A. A.; Abdou, A. Synthesis, characterization, and DFT study of linear and non-linear optical properties of some novel thieno [2, 3-b] thiophene azo dye derivatives. *Mater. Chem. Phys.* **2022**, *290*, No. 126646.
(33) Shebl, M.; Khalil, S. M. Synthesis, spectral, X-ray diffraction, antimicrobial studies, and DNA binding properties of binary and ternary complexes of pentadentate N 2 O 3 carbohydrazone ligands. *Monatsh. Chem.* **2015**, *146*, 15−33.
(34) Latif, M.; Ahmed, T.; Hossain, M. S.; Chaki, B.; Abdou, A.; Kudrat-E-Zahan, M. Synthesis, Spectroscopic Characterization, DFT Calculations, Antibacterial Activity, and Molecular Docking Analysis of Ni (II), Zn (II), Sb (III), and U (VI) Metal Complexes Derived from a Nitrogen-Sulfur Schiff Base. *Russ. J. Gen. Chem.* **2023**, *93*, 389−397.
(35) Morgan, S. M.; El-Sonbati, A.; Eissa, H. Geometrical structures, thermal properties and spectroscopic studies of Schiff base complexes: Correlation between ionic radius of metal complexes and DNA binding. *J. Mol. Liq.* **2017**, *240*, 752−776.
(36) Elkanzi, N. A.; Ali, A. M.; Albqmi, M.; Abdou, A. New Benzimidazole-Based Fe (III) and Cr (III) Complexes: Characterization, Bioactivity Screening, and Theoretical Implementations Using DFT and Molecular Docking Analysis. *Appl. Organomet. Chem.* **2022**, *36*, No. e6868.
(37) Prakash, A.; Singh, B. K.; Bhojak, N.; Adhikari, D. Synthesis and characterization of bioactive zinc (II) and cadmium (II) complexes with new Schiff bases derived from 4-nitrobenzaldehyde and acetophenone with ethylenediamine. *Spectrochim. Acta, Part A* **2010**, *76*, 356−362.
(38) Abdou, A. Synthesis, Structural, Molecular Docking, DFT, Vibrational Spectroscopy, HOMO-LUMO, MEP Exploration, anti-

https://doi.org/10.1021/acsomega.3c01413
ACS Omega 2023, 8, 25877−25891

bacterial and antifungal activity of new Fe (III), Co (II) and Ni (II) hetero-ligand complexes. *J. Mol. Struct.* **2022**, *1262*, No. 132911.
(39) Scholz, C.; Knorr, S.; Hamacher, K.; Schmidt, B. DOCKTITE— A Highly Versatile Step-by-Step Workflow for Covalent Docking and Virtual Screening in the Molecular Operating Environment. *J. Chem. Inf. Model.* **2015**, *55*, 398−406.
(40) Abd El-Lateef, H. M.; Khalaf, M. M.; Kandeel, M.; Amer, A. A.; Abdelhamid, A. A.; Abdou, A. Designing, Characterization, biological, DFT, and molecular docking analysis for new FeAZD, NiAZD, and CuAZD complexes incorporating 1-(2-hydroxyphenylazo)-2-naphthol (H2AZD). *Comput. Biol. Chem.* **2023**, *105*, No. 107908.
(41) Abd El-Lateef, H. M.; Khalaf, M. M.; Kandeel, M.; Amer, A. A.; Abdelhamid, A. A.; Abdou, A. New Mixed-ligand Thioether-quinoline complexes of Nickel (II), Cobalt (II), and Copper (II): Synthesis, Structural Elucidation, DFT, antimicrobial activity and Molecular docking exploration. *Appl. Organomet. Chem.* **2023**, *37*, No. e7134.
(42) Al-Ayash, S.; Al-Noor, T.; Abdou, A. Synthesis and Characterization of Metals Complexes with Uracil and Uracil Derivatives (A Review). *Russ. J. Gen. Chem.* **2023**, *93*, 987−995.
(43) Alghuwainem, Y. A.; El-Lateef, H. M. A.; Khalaf, M. M.; Amer, A. A.; Abdelhamid, A. A.; Alzharani, A. A.; Alfarsi, A.; Shaaban, S.; Gouda, M.; Abdou, A. Synthesis, DFT, Biological and Molecular Docking Analysis of Novel Manganese (II), Iron (III), Cobalt (II), Nickel (II), and Copper (II) Chelate Complexes Ligated by 1-(4-Nitrophenylazo)-2-naphthol. *Int. J. Mol. Sci.* **2022**, *23*, 15614.
(44) Al-Gaber, M. A. I.; Abd El-Lateef, H. M.; Khalaf, M. M.; Shaaban, S.; Shawky, M.; Mohamed, G. G.; Abdou, A.; Gouda, M.; Abu-Dief, A. M. Design, Synthesis, Spectroscopic Inspection, DFT and Molecular Docking Study of Metal Chelates Incorporating Azo Dye Ligand for Biological Evaluation. *Materials* **2023**, *16*, 897.
(45) Abdou, A.; Mostafa, H. M.; Abdel-Mawgoud, A.-M. M. Seven metal-based bi-dentate NO azocoumarine complexes: Synthesis, physicochemical properties, DFT calculations, drug-likeness, in vitro antimicrobial screening and molecular docking analysis. *Inorg. Chim. Acta* **2022**, *539*, No. 121043.
(46) Marković, M.; Judaš, N.; Sabolović, J. Combined Experimental and Computational Study of cis-trans Isomerism in Bis (l-valinato) copper (II). *Inorg. Chem.* **2011**, *50*, 3632−3644.
(47) Bacher, F.; Enyedy, E.; Nagy, N. R. V.; Rockenbauer, A.; Bognár, G. M.; Trondl, R.; Novak, M. S.; Klapproth, E.; Kiss, T. S.; Arion, V. B. Copper (II) complexes with highly water-soluble L-and D-Proline−thiosemicarbazone conjugates as potential inhibitors of topoisomerase IIα. *Inorg. Chem.* **2013**, *52*, 8895−8908.
(48) Shiju, C.; Arish, D.; Kumaresan, S. Synthesis, characterization, cytotoxicity, DNA cleavage, and antimicrobial activity of lanthanide (III) complexes of a Schiff base ligand derived from glycylglycine and 4-nitrobenzaldehyde. *Arab. J. Chem.* **2017**, *10*, S2584−S2591.
(49) Najar, A. M.; Eswayah, A.; Moftah, M. B.; Mk, R. O.; Bobtaina, E.; Najwa, M.; Elhisadi, T. A.; Tahani, A.; Tawati, S. M.; Khalifa, A. M. Rigidity and flexibility of pyrazole, s-triazole, and v-triazole derivative of chloroquine as potential therapeutic against COVID-19. *J. Med. Chem. Sci.* **2023**, *6*, 2056−2084.
(50) Ikram, M.; Rehman, S.; Faiz, A. Synthesis, characterization and antimicrobial studies of transition metal complexes of imidazole derivative. *Bull. Chem. Soc. Ethiop.* **2010**, *24*, 201.
(51) Aiyelabola, T.; Ojo, I.; Adebajo, A.; Ogunlusi, G.; Oyetunji, O.; Akinkunmi, E.; Adeoye, A. Synthesis, characterization and antimicrobial activities of some metal (II) amino acids' complexes. *Adv. Biol. Chem.* **2012**, *2*, 268.
(52) Fekri, A.; Zaky, R. Solvent-free synthesis and computational studies of transition metal complexes of the aceto-and thioaceto-acetanilide derivatives. *J. Organomet. Chem.* **2016**, *818*, 15−27.
(53) Kumar, A.; Kumar, D.; Kumari, K.; Mkhize, Z.; Seru, L. K.; Bahadur, I.; Singh, P. Metal-ligand complex formation between ferrous or ferric ion with syringic acid and their anti-oxidant and anti-microbial activities: DFT and molecular docking approach. *J. Mol. Liq.* **2021**, *322*, No. 114872.
(54) Hashem, H. E.; Nath, A.; Kumer, A. Synthesis, molecular docking, molecular dynamic, quantum calculation, and antibacterial activity of new Schiff base-metal complexes. *J. Mol. Struct.* **2022**, *1250*, No. 131915.
(55) Aljohani, E. T.; Shehata, M. R.; Alkhatib, F.; Alzahrani, S. O.; Abu-Dief, A. M. Development and structure elucidation of new VO2+, Mn2+, Zn2+, and Pd2+ complexes based on azomethine ferrocenyl ligand: DNA interaction, antimicrobial, antioxidant, anticancer activities, and molecular docking. *Appl. Organomet. Chem.* **2021**, *35*, No. e6154.
(56) Liu, J.-Q.; Chen, J.; Cheng, F.; Luo, D.; Huang, J.; Ouyang, J.; Nezamzadeh-Ejhieh, A.; Peng, Y.; Khan, M. S. Recent advances in Ti-based MOFs in the biomedical applications. *Dalton Trans.* **2022**, *51*, 14817.
(57) Al-Khateeb, Z. T.; Karam, F. F.; Al-Adilee, K. Synthesis and characterization of some metals complexes with new heterocyclic azo dye ligand 2-[2-(5-Nitro thiazolyl) azo]-4-methyl-5-nitro phenol and their biological activities. *J. Phys.: Conf. Ser.* **2019**, *1294*, No. 052043.
(58) Modhavadiya, V. Synthesis, characterization, spectral studies, biocidal activities of Fe (II) and Cu (II) complexes of azo dye ligand derived from sulfamethoxazole and substituted p-cresol. *Orient. J. Chem.* **2012**, *28*, 921.
(59) Rezaeivala, M.; Keypour, H. Schiff base and non-Schiff base macrocyclic ligands and complexes incorporating the pyridine moiety−The first 50 years. *Coord. Chem. Rev.* **2014**, *280*, 203−253.
(60) Job, P. Recherches sur la formation de complexes minéraux en solution, et sur leur stabilité. *Ann. Chim.* **1928**, *9*, 113−203.
(61) Fan, R.; Sumitani, R.; Mochida, T. Synthesis and Reactivity of Cyclopentadienyl Ruthenium (II) Complexes with Tris (alkylthio) benzenes: Transformation between Dinuclear and Sandwich-Type Complexes. *ACS Omega* **2020**, *5*, 2034−2040.
(62) Arafath, M. A.; Adam, F.; Ahamed, M. B. K.; Karim, M. R.; Uddin, M. N.; Yamin, B. M.; Abdou, A. Ni (II), Pd (II) and Pt (II) complexes with SNO-group thiosemicarbazone and DMSO: Synthesis, characterization, DFT, molecular docking and cytotoxicity. *J. Mol. Struct.* **2023**, *1278*, No. 134887.
(63) Rahmouni, N. T.; el Houda Bensiradj, N.; Megatli, S. A.; Djebbar, S.; Baitich, O. B. New mixed amino acids complexes of iron (III) and zinc (II) with isonitrosoacetophenone: Synthesis, spectral characterization, DFT study and anticancer activity. *Spectrochim. Acta, Part A* **2019**, *213*, 235−248.
(64) Parr, R. G.; Yang, W. Density functional approach to the frontier-electron theory of chemical reactivity. *J. Am. Chem. Soc.* **1984**, *106*, 4049−4050.
(65) Yu, J.; Su, N. Q.; Yang, W. Describing Chemical Reactivity with Frontier Molecular Orbitalets. *JACS Au* **2022**, *2*, 1383−1394.
(66) Hrichi, H.; Elkanzi, N. A.; Ali, A. M.; Abdou, A. A novel colorimetric chemosensor based on 2-[(carbamothioylhydrazono) methyl] phenyl 4-methylbenzenesulfonate (CHMPMBS) for the detection of Cu (II) in aqueous medium. *Res. Chem. Intermed.* **2023**, *49*, 2257−2276.
(67) Hossain, M.; Khushy, K.; Latif, M.; Hossen, M. F.; Asraf, M. A.; Kudrat-E-Zahan, M.; Abdou, A. Co (II), Ni (II), and Cu (II) Complexes Containing Isatin-Based Schiff Base Ligand: Synthesis, Physicochemical Characterization, DFT Calculations, Antibacterial Activity, and Molecular Docking Analysis. *Russ. J. Gen. Chem.* **2022**, *92*, 2723−2733.
(68) Abu-Dief, A. M.; Alotaibi, N. H.; Al-Farraj, E. S.; Qasem, H. A.; Alzahrani, S.; Mahfouz, M. K.; Abdou, A. Fabrication, structural elucidation, theoretical, TD-DFT, vibrational calculation and molecular docking studies of some novel adenine imine chelates for biomedical applications. *J. Mol. Liq.* **2022**, *365*, No. 119961.
(69) Abdou, A.; Abdel-Mawgoud, A. M. M. Synthesis, structural elucidation, and density functional theory investigation of new mononuclear Fe (III), Ni (II), and Cu (II) mixed-ligand complexes: Biological and catalase mimicking activity exploration. *Appl. Organomet. Chem.* **2022**, *36*, No. e6600.
(70) Abdou, A.; Omran, O. A.; Nafady, A.; Antipin, I. S. Structural, spectroscopic, FMOs, and non-linear optical properties exploration of three thiacaix (4) arenes derivatives. *Arab. J. Chem.* **2022**, *15*, No. 103656.

https://doi.org/10.1021/acsomega.3c01413
ACS Omega 2023, 8, 25877−25891

(71) Chattaraj, P. K.; Roy, D. R. Update 1 of: electrophilicity index. *Chem. Rev.* **2007**, *107*, PR46−PR74.
(72) Khan, I. M.; Shakya, S. Exploring colorimetric real-time sensing behavior of a newly designed CT complex toward nitrobenzene and Co2+: spectrophotometric, DFT/TD-DFT, and mechanistic insights. *ACS Omega* **2019**, *4*, 9983−9995.
(73) Varukolu, M.; Palnati, M.; Nampally, V.; Gangadhari, S.; Vadluri, M.; Tigulla, P. New Charge Transfer Complex between 4-Dimethylaminopyridine and DDQ: Synthesis, Spectroscopic Characterization, DNA Binding Analysis, and Density Functional Theory (DFT)/Time-Dependent DFT/Natural Transition Orbital Studies. *ACS Omega* **2022**, *7*, 810−822.
(74) Ouaket, A.; Chraka, A.; Raissouni, I.; El Amrani, M. A.; Berrada, M.; Knouzi, N. Synthesis, spectroscopic (13C/1H-NMR, FT-IR) investigations, quantum chemical modelling (FMO, MEP, NBO analysis), and antioxidant activity of the bis-benzimidazole molecule. *J. Mol. Struct.* **2022**, *1259*, No. 132729.
(75) Gadhe, C. G.; Kothandan, G.; Cho, S. J. Large variation in electrostatic contours upon addition of steric parameters and the effect of charge calculation schemes in CoMFA on mutagenicity of MX analogues. *Mol. Simul.* **2012**, *38*, 861−871.
(76) Kargar, H.; Fallah-Mehrjardi, M.; Behjatmanesh-Ardakani, R.; Munawar, K. S. Synthesis, spectra (FT-IR, NMR) investigations, DFT, FMO, MEP, NBO analysis and catalytic activity of MoO2 (VI) complex with ONO tridentate hydrazone Schiff base ligand. *J. Mol. Struct.* **2021**, *1245*, No. 131259.
(77) Weinhold, F.; Landis, C. R. Natural bond orbitals and extensions of localized bonding concepts. *Chem. Educ. Res. Pract.* **2001**, *2*, 91−104.
(78) Tanak, H.; Ağar, A.; Yavuz, M. Combined experimental and computational modeling studies on 4-[(2-hydroxy-3-methylbenzylidene) amino]-1, 5-dimethyl-2-phenyl-1, 2-dihydro-3H-pyrazol-3-one. *Int. J. Quantum Chem.* **2011**, *111*, 2123−2136.
(79) Premkumar, S.; Jawahar, A.; Mathavan, T.; Dhas, M. K.; Sathe, V.; Benial, A. M. F. DFT calculation and vibrational spectroscopic studies of 2-(tert-butoxycarbonyl (Boc)-amino)-5-bromopyridine. *Spectrochim. Acta, Part A* **2014**, *129*, 74−83.
(80) Premkumar, S.; Rekha, T.; Rajkumar, B. J.; Asath, R. M.; Jawahar, A.; Mathavan, T.; Benial, A. M. F. Vibrational spectroscopic and structural investigations of 2-amino-6-methoxy-3-nitropyridine: a DFT approach. *Braz. J. Phys.* **2015**, *45*, 621−632.
(81) Schatz, A.; Martin, J. J.; Fosdick, L.; Leicester, H. M. The proteolysis-chelation theory of dental caries. *J. Am. Dent. Assoc.* **1962**, *65*, 368−375.
(82) Wang, X. A chelate theory for the mechanism of action of aspirin-like drugs. *Med. Hypotheses* **1998**, *50*, 239−251.
(83) Kubota, Y.; Tanaka, S.; Funabiki, K.; Matsui, M. Synthesis and fluorescence properties of thiazole−boron complexes bearing a β-ketoiminate ligand. *Org. Lett.* **2012**, *14*, 4682−4685.
(84) Skotnicka, A.; Kolehmainen, E.; Czeleń, P.; Gawinecki, R.; Valkonen, A. Tautomeric equilibria in solutions of 2-phenacylbenzoxazoles. *Int. J. Mol. Sci.* **2013**, *14*, 4444−4460.
(85) Rahimizadeh, M.; Eshghi, H.; Shiri, A.; Ghadamyari, Z.; Matin, M. M.; Oroojalian, F.; Pordeli, P. Fe (HSO 4) 3 as an efficient catalyst for diazotization and diazo coupling reactions. *J. Korean Chem. Soc.* **2012**, *56*, 716−719.
(86) Shomali, A.; Valizadeh, H.; Noorshargh, S. New Generation of Nitrite Functionalized Star-like Polyvinyl Imidazolium Compound: Application as a Nitrosonium Source and Three Dimensional Nanocatalyst for the Synthesis of Azo Dyes. *Lett. Org. Chem.* **2017**, *14*, 409−418.
(87) Akki, M.; Reddy, D. S.; Katagi, K. S.; Kumar, A.; Devarajegowda, H. C.; Babagond, V.; Mane, S.; Joshi, S. D. Synthesis of coumarin-thioether conjugates as potential anti-tubercular agents: Their molecular docking and X-ray crystal studies. *J. Mol. Struct.* **2022**, *1266*, No. 133452.
(88) Perveen, F.; Qureshi, R.; Ansari, F. L.; Kalsoom, S.; Ahmed, S. Investigations of drug−DNA interactions using molecular docking, cyclic voltammetry and UV−Vis spectroscopy. *J. Mol. Struct.* **2011**, *1004*, 67−73.
(89) Deghadi, R. G.; Abbas, A. A.; Mohamed, G. G. Theoretical and experimental investigations of new bis (amino triazole) schiff base ligand: Preparation of its UO2 (II), Er (III), and La (III) complexes, studying of their antibacterial, anticancer, and molecular docking. *Appl. Organomet. Chem.* **2021**, *35*, No. e6292.
(90) Jarad, A. J.; Dahi, M. A.; Al-Noor, T. H.; El-ajaily, M. M.; AL-Ayash, S. R.; Abdou, A. Synthesis, spectral studies, DFT, biological evaluation, molecular docking and dyeing performance of 1-(4-((2-amino-5-methoxy) diazenyl) phenyl) ethanone complexes with some metallic ions. *J. Mol. Struct.* **2023**, *1287*, No. 135703.
(91) Murugan, T.; Venkatesh, R.; Geetha, K.; Abdou, A. Synthesis, Spectral Investigation, DFT, Antibacterial, Antifungal and Molecular Docking Studies of Ni(II), Zn(II), Cd(II) Complexes of Tetradentate Schiff-Base Ligand. *Asian J. Chem.* **2023**, *35*, 1509−1517.
(92) Elkanzi, N. A.; Ali, A. M.; Hrichi, H.; Abdou, A. New mononuclear Fe (III), Co (II), Ni (II), Cu (II), and Zn (II) complexes incorporating 4-{[(2 hydroxyphenyl) imino] methyl} phenyl-4-methylbenzenesulfonate (HL): Synthesis, characterization, theoretical, anti-inflammatory, and molecular docking investigation. *Appl. Organomet. Chem.* **2022**, *36*, No. e6665.
(93) Shaaban, S.; Abdou, A.; Alhamzani, A. G.; Abou-Krisha, M. M.; Al-Qudah, M. A.; Alaasar, M.; Youssef, I.; Yousef, T. A. Synthesis and in silico investigation of organoselenium-clubbed schiff bases as potential Mpro inhibitors for the SARS-CoV-2 replication. *Life* **2023**, *13*, 912.

https://doi.org/10.1021/acsomega.3c01413
ACS Omega 2023, 8, 25877−25891